Characterization of Human DNase I Family Endonucleases and Activation of DNase γ during Apoptosis[†]

Daisuke Shiokawa[‡] and Sei-ichi Tanuma*[,‡,§]

Department of Biochemistry, Faculty of Pharmaceutical Sciences, Science University of Tokyo, 12 Funagawara-machi, Ichigaya, Shinjuku-ku, Tokyo 162-0826, Japan, and Research Institute for Bioscience, Science University of Tokyo, 2669 Yamazaki, Noda, Chiba 278-0022, Japan

Received May 8, 2000; Revised Manuscript Received October 17, 2000

ABSTRACT: We describe here the characterization of the so far identified human DNase I family DNases, DNase I, DNase X, DNase γ, and DNAS1L2. The DNase I family genes are found to be expressed with different tissue specificities and suggested to play unique physiological roles. All the recombinant DNases are shown to be Ca^{2+}/Mg^{2+}-dependent endonucleases and catalyze DNA hydrolysis to produce 3′-OH/5′-P ends. High activities for DNase I, DNase X, and DNase γ are observed under neutral conditions, whereas DNAS1L2 shows its maximum activity at acidic pH. These enzymes have also some other peculiarities: different sensitivities to G-actin, aurintricarboxylic acid, and metal ions are observed. Using a transient expression system in HeLa S3 cells, the possible involvement of the DNases in apoptosis was examined. The ectopic expression of each DNase has no toxic effect on the host cells; however, extensive DNA fragmentation is observed only in DNase γ-transfected cells after the induction of apoptosis. Furthermore, DNase γ is revealed to be located at the perinuclear region in living cells, and to translocate into the nucleus during apoptosis. Our results demonstrate that DNase I, DNase X, DNase γ, and DNAS1L2 have similar but unique endonuclease activities, and that among DNase I family DNases, DNase γ is capable of producing apoptotic DNA fragmentation in mammalian cells.

DNase I is one of the most characterized mammalian endonucleases. It was originally identified as a pancreatic enzyme that catalyzes DNA hydrolysis in the presence of appropriate divalent cations (*1*). DNase I has been purified from various mammalian tissues and body fluids, and its characterization has revealed that DNase I is an endonuclease that exerts its full activity in the presence of both Ca^{2+} and Mg^{2+} under neutral pH conditions (*1*−*3*). Most of the neutral divalent cation-dependent DNase activities so far detected in various tissues or cells have been recognized as DNase I. However, the existence of several DNase I-like human genes/proteins has recently been reported, namely, DNase X/Xib (*5*, *6*), DNase γ/DNAS1L3/LS-DNase (*7*−*9*), and DNAS1L2 (*8*).

Among DNase I family DNases, the physical and enzymatic properties of DNase I and DNase γ have been extensively characterized (*1*−*3*, *10*−*12*). Although some differences are found in their properties, these two DNases share many common features: (i) high activities are observed under neutral pH, (ii) Ca^{2+} and Mg^{2+} activate both in a synergistic manner, and (iii) they cleave DNA endonucleolitically to produce 3′-OH/5′-P ends. Although the enzymatic properties of DNase X and DNAS1L2 are at present unclear, they are suggested to have DNase I or DNase γ-like DNase activities on the basis of their well-conserved primary structures. Two groups have succeeded in generating recombinant DNase X protein using bacterial expression systems and have examined its DNase activity independently. However, their results are quite different: one group identified DNase X as a Ca^{2+}/Mg^{2+}-dependent endonuclease (*5*), whereas the other reported it to show a divalent cation-independent acid endonuclease activity (*13*). On the other hand, no reports on physical or enzymatic properties of the DNAS1L2 protein have been published.

Although the physiological significance of DNase I family DNases is yet to be fully understood, DNase I and DNase γ have been suggested to be involved in apoptosis (*14*−*20*). Apoptosis is a form of cell death by which unwanted or potentially harmful cells are eliminated under a wide variety of physiological and pathological situations (*21*, *22*). After the induction of apoptosis, dying cells are quickly engulfed and degraded by neighboring cells or macrophages in vivo (*21*). In a nematode *Caenorhabditis elegans*, it has been known that the DNA of engulfed cells is degraded by a DNase controlled by *nuc-1* gene (*23*). Very recently, the *nuc-1* gene has been shown to encode a homologue of mammalian acidic endonuclease, DNase II, and to mediate the conversion of TUNEL-reactive DNA into TUNEL-unreactive DNA in dying cells (*24*). In accordance with this finding, a role for DNase II in the degradation of DNA of engulfed cells has also been suggested in mammalian apoptotic systems (*25*, *26*).

[†] This work was supported in part by a Grant-in-Aid for Scientific Research from the Ministry of Education.

* To whom correspondence should be addressed at the Department of Biochemistry, Faculty of Pharmaceutical Sciences, Science University of Tokyo, 12 Funagawara-machi, Ichigaya, Shinjuku-ku, Tokyo 162-0826, Japan. Telephone: +81-3-3260-6725; Fax: +81-3-3268-3045; E-mail: tanuma@ps.kagu.sut.ac.jp.

[‡] Department of Biochemistry, Science University of Tokyo.

[§] Research Institute for Bioscience, Science University of Tokyo.

10.1021/bi001041a CCC: $20.00
Published on Web 12/09/2000

Besides the DNA degradation by phagocytes, apoptotic cells cleave their own genomic DNA into oligonucleosomal fragments. The process, known as apoptotic DNA fragmentation, has been recognized as one of the outstanding features of mammalian apoptosis (*27*, *28*). Many efforts have been made to identify the DNase(s) responsible for this process and, at present, several DNases, including DNase I, DNase γ, DNase II, L-DNase II, and CAD/DFF40/CPAN, are considered to be candidates (*14*−*20*, *29*−*35*). Among these, the regulatory mechanism of the CAD activity has been well-established (*32*), and its involvement in Fas-induced apoptosis in Jurkat cells and dexamethasone-induced thymic apoptosis has been demonstrated (*36*, *37*). However, evidence supporting the involvement of other candidates, including DNase I and DNase γ, is also accumulating (*14*−*20*, *29*−*31*). Thus, the DNase(s) involved in apoptotic DNA fragmentation is considered to differ in cell types, differentiation status, and/or apoptotic stimuli, and the identification of the responsible DNase(s) in each apoptotic case remains controversial.

DNases have recently attracted attention with regard to their clinical application as therapy for cystic fibrosis (CF),[1] a lethal disease common in Caucasian populations (*38*, *39*). Human recombinant DNase I has recently been approved as a therapy to improve the lung function of CF patients, because the viscoelastic nature of CF sputum is contributed to by the high concentration of DNA released by dead leukocytes (*38*, *39*). Thus, the physiological and clinical importance of the DNase I family DNases is now being recognized and is becoming a focus of research.

The aim of this study is to examine and compare the physical and enzymatic properties of the four DNase I family DNases and to assess their possible involvement in DNA fragmentation during apoptosis.

MATERIALS AND METHODS

Construction of Expression Vectors. Human cDNA fragments containing open reading frames (without stop codons) of DNase I, DNase X, DNase γ, and DNAS1L2 were generated by PCR from liver, HeLa S3 cells, spleen, and fetal brain cDNA libraries, respectively, and subcloned into pBluescript KS+. The primers used were DNase I, 5′-**CTCGAG**CCACCATGAGGGGCATGAAGCTGCTG-3′ (sense) and 5′-**CTCGAG**ACTTCAGCATCACCTCCACTG-3′ (antisense); DNase X, 5′-**CTCGAG**CCACCATGCACTACCCAACTGCAC-3′ (sense) and 5′-**CTCGAG**AGGCAGCAGGGCACAGCTGA-3′ (antisense); DNase γ, 5′-**CTCGAG**CCACCATGTCACGGGAGCTGGCCCCA-3′ (sense) and 5′-**CTCGAG**GGAGCGTTTGCTCTTTGTTTTC-3′ (antisense); DNAS1L2, 5′-**CTCGAG**CCACCATGGGCGGGCCCCGGGCT-3′ (sense) and 5′-**CTCGAG**ATCGGTGGAACTTGAGGGTCAC-3′ (antisense). *Xho*I sites flanking the coding sequences are shown in bold face. After confirming the sequences, the inserts were excised by *Xho*I digestion and recloned into the *Xho*I site of pcDNA3-Myc-His C (Invitrogen) to generate expression vectors for C-terminal Myc and His tagged forms of DNase I (phDNase I-Myc-His), DNase X (phDNase X-Myc-His), DNase γ (phDNase γ-Myc-His), and DNAS1L2 (phDNAS1L2-Myc-His). In the construction of DNase γ-GFP and DNAS1L2-GFP chimeric protein expression vectors (phDNase γ-GFP and phDNAS1L2-GFP, respectively), *Xho*I cDNA fragments for each DNase were recloned into the *Xho*I site of pEGFP-N3 (Clontech).

Transfection and Purification of Recombinant Human DNases. Human embryonic kidney 293 cells (5×10^6), grown in DMEM supplemented with 10% fetal calf serum, were transfected with 25 μg of each expression vector using a FuGene 6 transfection reagent (Boehringer). The cells were harvested 48 h after transfection and homogenized in 2 mL of ice-cold buffer A [10 mM Tris-HCl (pH 7.8), 3 mM $MgCl_2$, 1 mM 2-mercaptoethanol, 0.3 mM PMSF] containing 0.1% Nonidet P-40 and 0.3 M NaCl by10 strokes of a Teflon-glass homogenizer. The homogenate was centrifuged at 10000*g* for 10 min, and the supernatant was collected as the cell extract. His-tagged recombinant protein was purified from the cell extract with Ni-NTA magnetic beads (Qiagen) according to the manufacturer's protocol. Purified recombinant DNases, eluted in 100 μL of elution buffer [50 mM sodium phosphate (pH 8.0) containing 250 mM imidazole and 300 mM NaCl], were dialyzed against 20 mM Mes-NaOH (pH 5.6) containing 1 mM 2-mercaptoethanol, and BSA was added to a final concentration of 0.1 mg/mL. These enzyme preparations were used to characterize DNase activities.

RNA Dot Blot Analysis. The expression of DNases in adult and fetal human tissues was examined using Human RNA Master Blot (Clontech) according to the manufacturer's protocol. cDNA fragments encoding each DNase were excised from their expression vectors by *Xho*I digestion, labeled with ^{32}P, and used as probes. After hybridization, the blots were washed, the autoradiograms were visualized, and the intensity of each dot was quantified using a BAS 1500 imaging system (Fuji Film). The expression level of each gene was normalized to 100% for DNase I expression level in pancreas and described as follows: +++, over 60%; ++, between 30% and 60%; +, less than 30%; −, not detected. Signals detected in human genomic DNA were used for interblot normalization.

RT-PCR Analysis. RT-PCR analysis was performed using total RNA extracted from HeLa S3 cells as described previously (*17*). PCR amplification was carried out by 30 cycles; each cycle consisted of denaturation at 94 °C for 30 s, annealing at 62 °C for 30 s, and extension at 72 °C for 1 min. The primers used were DNase II (349 bp), (sense) 5′-GCTTCTGGCTGGTCCACAGTG-3′ and (antisense) 5′-CCGGAGTACAGGTCATCTCCA-3′; DFF40/CAD (542 bp), (sense) 5′-GCCTGTACGAGGATGGCACGG-3′ and (antisense) 5′-CTGGCAGGAGAACCAGCCTTC-3′; DFF45/ICAD (772 bp), (sense) 5′-GGCCATTGATAAGTCCCTGAC-3′ and (antisense) 5′-CCGGAGAGAATGCAAGCTCTG-3′; DNase I (322 bp), (sense) 5′-GACGGAACAGCTATAAGGAGC-3′ and (antisense) 5′-GAGGGTCTCACATAGCTGCAG-3′; DNase X (313 bp), (sense) 5′-CGATGTGTTTCTGGAGGTCTC-3′ and (antisense) 5′-GTAGTGGTCACTGATGTTGAGG-3′; DNase γ (360 bp), (sense) 5′-CTATGTGATTAGCTCTCGGCTTGGAAG-3′ and (anti-

[1] Abbreviations: Act D, actinomycin D; ATA, aurintricarboxylic acid; BFP, blue fluorescent protein; CF, cystic fibrosis; ER, endoplasmic reticulum; EST, expressed sequence tag; GFP, green fluorescent protein; NLS, nuclear localization signal; ORF, open reading frame; PI, propidium iodide; RT-PCR, PCR-mediated amplification of reverse transcribed mRNA; TUNEL, terminal deoxynucleotidyl transferase-mediated nick end-labeling.

sense) 5′-CGGATGTTCTTCCAGGCCTTCTTGGGG-3′; DNAS1LS (393 bp), (sense) 5′-GATGTACCTGTTCGTGTACAGG-3′ and (antisense) 5′-CACTTGAAGACCTCACTGCTC-3′; GAPDH (452 bp), (sense) 5′-ACCACAGTCCATGCCATCAC-3′ and (antisense) 5′-TCCACCACCCTGTTGCTGTA-3′.

Western Blot Analysis. 293 cells (2×10^5) were transfected individually with 1 μg of each expression vector as described above. The cells were cultured in 2 mL of DMEM supplemented with 10% fetal calf serum for 48 h, and the culture medium and cells were collected separately. Aliquots of the medium (100 μL) or cells (2×10^5) were subjected to 12% SDS−PAGE and transferred onto nitrocellulose membranes. Blots were probed with anti-Myc antibody (Novagen) as described previously (*40*).

Assay of DNase Activity. A total of 20 μL of reaction mixture [50 mM Mes-NaOH or Mops-NaOH, 0.3−3 mM $CaCl_2$ (see below), 3 mM $MgCl_2$, 1 mM 2-mercaptoethanol, 1 unit of enzyme, and 500 ng Eco RI-digested linear pBluescript II KS+] was prepared on ice and incubated at 37 °C for 20 min. In the standard assays of each DNase, the following buffers ($CaCl_2$ concentration) were used: DNase I, Mops-NaOH, pH 6.8 (0.3 mM); DNase X, Mops-NaOH, pH 6.8 (1 mM); DNase γ, Mops-NaOH, pH 7.2 (3 mM); DNAS1L2, Mes-NaOH, pH 5.6 (3 mM). In this study, one unit of DNase activity is defined as the amount required to cause a decrease in band intensity corresponding to 200 ng of intact substrate in each standard assay. DNase activities were quantified by the reduction of the band intensities of intact substrate as described previously (*40*). Alternatively, DNase activities were assayed using supercoiled plasmid to show their endonuclease activities (Figure 3). In these cases, 2 units of enzymes was used in the reactions to obtain clear results.

End-Labeling of DNA. The cleaved ends of the DNA digested by each DNase were analyzed by 3′- and 5′- end-labeling as described previously (*40*). In brief, the 3′-ends of the DNA fragments were labeled by [α-^{32}P]dCTP with terminal deoxynucleotidyl transferase (Toyobo), and the 5′-ends were labeled by [γ-^{32}P]ATP with polynucleotide kinase (Toyobo). The phosphoryl groups at the ends of the DNA chains were removed by pretreatment with calf intestine alkaline phosphatase (Takara). The resulting labeled DNAs were subjected to 1% agarose gel electrophoresis, transferred to a nylon membrane, and analyzed with a BAS 1500 image analyzer (Fuji Film).

Induction and Detection of Apoptosis. Human cervix adenocarcinoma HeLa S3 cells (2×10^5) were cotransfected with pEBFP-C1 (0.5 μg) and expression vectors for each DNase (0.5 μg) as described above. At 48 h post-transfection, the culture medium was replaced with fresh medium, and apoptosis was induced with TNF-α (1 ng/mL) in the presence of Act D (0.3 μg/mL). Cells were harvested after 12 h incubation, and the frequencies of apoptotic cells were determined on BFP-positive cells by fluorescence microscopy using Annexin V-FITC Apoptosis Detection kit (MBL) according to the manufacturer's protocol. Values are the averages of three independent experiments, and at least 400 cells were counted in each sample. Annexin V interacts with the externalized phosphatidylserine, an early marker for apoptosis, and PI staining detects loss of membrane integrity, a feature for the late stage of apoptosis. DNA fragmentation

```
DNase I   -22  MRGMK-LLGALLALAALLQGAVSLKIAAFNIQTFGETKMSNATLVSYIVQ
DNase X   -18  MHYPTALL-----FLILANGAQAFRICAFNAQRLTLAKVAREQVMDTLVR
DNase γ   -20  MSRE---LAPLLLLLLSIHSALAMRICSFNVRSFGESKQEDKNAMDVIVK
DNAS1L2   -18  MGGPRALLAALWALEA--AGTAALRIGAFNIQSFGDSKVSDPACGSIIAK
               *      *     .     .. . .* .** . .  .*          . .

DNase I    28  ILSRYDIALVQEVRDSHLTAVGKLLDNLNQDAPD--TYHYVVSEPLGRNS
DNase X    28  ILARCDIMVLQEVVDSSGSAIPLLLRELNRFDGSG-PYSTLSSPQLGRST
DNase γ    28  VIKRCDIILVMEIKDSNNRICPILMEKLNRNSRRGITYNYVISSRLGRKT
DNAS1L2    31  ILAGYDLALVQEVRDPDLSAVSALMEQINSVSEH--EYSFVSSQPLGRDQ
               ..   *. .. *. *.       *.  .*        *  . *  ***

DNase I    76  YKERYLFVYRPDQVSAVDSYYYDDGCEPCGNDTFNREPAIVRFFSRFTEV
DNase X    77  YMETYVYFYRSHKTQVLSSYVYND-----EDDVFAREPFVAQFSLPSNVL
DNase γ    78  YKEQYAFLYKEKLVSVKRSYHYHD-YQDGDADVFSREPFVVWFQSPHTAV
DNAS1L2    79  YKEMYLFVYRKDAVSVVDTYLYPDP-----EDVFSREPFVVKFSAPGTGE
               * * * . *.        .* * *       * * *** .  *

DNase I   126  R--------------------EFAIVPLHAAPGDAVAEIDALYDVYLDVQ
DNase X   122  P--------------------SLVLVPLHTTPKAVEKELNALYDVFLEVS
DNase γ   127  K--------------------DFVIIPLHTTPETSVKEIDELVEVYTDVK
DNAS1L2   124  RAPPLPSRRALTPPPLPAAAQNLVLIPLHAAPHQAVAEIDALYDVYLDVI
                                    . ..***..*     *.. * .*. .*

DNase I   156  EKWGLEDVMLMGDFNAGCSYVRPSQWSSIRLWTSPTFQWLIPDSADTTAT
DNase X   152  QHWQSKDVILLGDFNADCASLTKKRLDKLELRTEPGFHWVIADGEDTTVR
DNase γ   157  HRWKAENFIFMGDFNAGCSYVPKKAWKNIRLRTDPRFVWLIGDQEDTTVK
DNAS1L2   174  DKWGTDDMLFLGDFNADCSYVRAQDWAAIRLRSSEVFKWLIPDSADTTVG
               . *   . ...*****.*. .       . *..   * *.* *  ***

DNase I   206  -PTHCAYDRIVVAGMLLRGAVVPDSALPFNFQAAYGLSDQLAQAISDHYP
DNase X   202  ASTHCTYDRVVLHGERCRSLL--HTAAAFDFPTSFQLTEEEALNISDHYP
DNase γ   207  KSTNCAYDRIVLRGQEIVSSVVPKSNSVFDFQKAYKLTEEEALDVSDHFP
DNAS1L2   224  -NSDCAYDRIVACGARLRRSLKPQSATVHDFQEEFGLDQTQALAISDHFP
                 ..*.***.*  *      .   .    .*   . * .  *  .***.*

DNase I   255  VEVMLK-----------------------------
DNase X   250  VEVELKLSQAHSVQPLSLTVLLLLSLLSPQLCPAA
DNase γ   257  VEFKLQSSRAFTNSKKSVTLRKKTKSKRS------
DNAS1L2   273  VEVTLKFHR---------------------------
               **  *.
```

FIGURE 1: Comparison of the amino acid sequences of human DNase I family DNases. Sequence alignment of human DNase I, DNase X, DNase γ, and DNAS1L2 proteins were performed using the Clustal V program. Identical and conserved residues are indicated by asterisks and dots, respectively. Dashes indicate gaps introduced for better alignment. Putative signal sequences/precursor peptides, predicted by PSORT II program, are shaded. Two conserved His residues (possible active sites) are shown by bold letters. Potential Asn-linked glycosylation sites are outlined. Possible nuclear localization signals of DNase γ, bipartite type (N-terminal half) and basic domain (C-terminal), are underlined. Amino acid numbers are shown at the left. Amino acid numbering begins at the N-terminal postulated for the mature enzymes with negative numbers for the precursor peptides (shaded). The GenBank accession numbers of human DNase I, DNase X, DNase γ, and DNAS1L2 are M55983, X90392, U75744, and U62647, respectively.

was analyzed by 2% agarose gel electrophoresis as described previously (*41*).

Subcellular Localization of DNase γ-GFP Protein. 2×10^5 HeLa S3 cells, grown on a coverslip, were transfected with 1 μg of phDNase γ-GFP or phDNAS1L2-GFP as described above. Cells were cultured for 48 h, and apoptosis was induced with TNF-α/Act D as described above. After 12 h incubation, cells were fixed with 1% glutaraldehyde at room temperature for 10 min, washed with PBS(−), and counterstained with 1 mM Hoechst 33258. The GFP and DNA images were observed by fluorescence microscopy (Olympus).

RESULTS

Sequence Comparison of Human DNase I Family Proteins. To date, four distinct human DNase I-like genes have been identified; the deduced amino acid sequences of their coding proteins, DNase I, DNase X, DNase γ, and DNAS1L2, are summarized in Figure 1. As a common structural feature, all the DNase I family proteins contain hydrophobic signal/precursor peptides in their N-termini, suggesting their

localization outside of the cell, including the inner space of organella such as ER, Golgi, and the nuclear envelope. In DNase I and DNase γ, these domains have been shown to be precursor peptides removed in the mature proteins (*4*, *17*). Furthermore, the peptide of DNase I works as a signal sequence for the extracellular secretion of the protein (*4*). Consistent with its extracellular secretion, DNase I has two potential *N*-linked glycosylation motifs (Figure 1, outlined), and Asn 18 has been shown to be glycosylated in bovine DNase I (*42*). Among the other members, DNase X contains one potential *N*-linked glycosylation site at Asn 243 (Figure 1, outlined). No Asn-X-Thr/Ser motif is found in DNase γ or DNAS1L2.

DNase X and DNase γ have unique extra-stretches in their C-termini. The hydrophobic stretch of DNase X and the basic domain of DNase γ have been predicted to be a membrane-anchoring peptide and a nuclear localization signal (NLS) (Figure 1, underlined), respectively (*17*, *43*). In addition to the C-terminal NLS, DNase γ contains potential bipartite type NLS in its N-terminal half (Figure 1, underlined).

Expression of the DNase I Family Genes. We performed poly A(+) RNA dot blot hybridization to determine the expression of the DNase I-like genes in 50 adult and fetal human tissues. The resulting autoradiograms were analyzed by densitometry, and the results are summarized in Table 1.

DNase I family genes are found to be expressed in a wide variety of human tissues; however, high levels of expression of each gene are found to be limited to specific tissues: DNase I in pancreas, kidney, and small intestine; DNase X in heart and skeletal muscle; and DNase γ in pituitary gland, adrenal grand, liver, spleen, and bone marrow (Table 1). The level of expression of the DNAS1L2 gene is extremely low; however, its transcript is detected in several tissues including colon, lung, and placenta. During our search using the Expressed Sequence Tag (EST) database, several EST clones for DNAS1L2 were found in skin-derided cDNA libraries (data not shown), suggesting that the DNAS1L2 gene may be highly expressed in skin.

Expression of Recombinant DNase I Family Proteins in Cultured Human Cells. We expressed DNase I family proteins as C-terminal Myc-His-tagged forms in 293 cells and detected them by Western blot probed with anti-Myc antibody. Because their conserved potential signal sequences predict the extracellular secretion of the proteins, we performed Western analysis also on the culture medium. Among the DNase I-like proteins, DNase I and DNAS1L2 were detected in the culture medium, and in comparison, DNase I was found to be secreted more efficiently than DNAS1L2 (Figure 2). The 37-kDa DNase I band was detected in both the cellular and the extracellular fractions. The apparent M_r of DNase I is higher than its calculated M_r of 32 498. In this section, the calculated M_r of each DNase includes the values for C-terminal Myc and His tags but not each precursor peptide. This is likely to be due to multiple glycosylation of the DNase I when it is expressed in mammalian cells (*44*). Like DNase I, the DNAS1L2 was detected in both the cellular and the extracellular fractions; however, two bands could be seen in the cellular fraction. The apparent M_r of the upper band (35 kDa) is in agreement with the calculated M_r (34347); however, the M_r of the lower band (32 kDa) was estimated to be lower than the calculated M_r. The apparent M_r of the extracellular band was the same as this lower band. At present, the reason why the short form of DNAS1L2 is produced in this system is unknown.

Table 1: Expression levels of DNase I Family Genes

Tissues	Expression Level [a]			
	DNase I	DNase X	DNase γ	DNAS1L2
whole brain	–	–	–	–
amygdala	–	+	–	+
caudate nucleus	–	–	–	–
cerebellum	–	–	–	–
cerebral cortex	–	–	–	–
frontal lobe	–	–	–	–
hippocampus	–	–	–	–
medulla oblongata	–	–	–	–
occipital lobe	–	–	–	+
putamen	–	+	–	+
substantia nigra	+	+	–	–
temporal lobe	+	+	–	+
thalamus	–	+	–	+
nucleus accumbeus	–	+	–	+
spinal cord	–	+	+	+
heart	+	++	–	–
aorta	+	+	+	–
skeletal muscle	+	+++	–	+
colon	+	+	+	–
bladder	–	+	+	–
uterus	+	+	+	–
prostate	+	+	+	+
stomach	+	+	+	+
testis	+	+	+	–
ovary	+	+	–	+
pancreas	+++	+	–	+
pituitary gland	+	+	+++	+
adrenal gland	+	+	+++	+
thyroid gland	+	+	+	+
salivary gland	+	+	+	+
mammary gland	+	+	+	+
kidney	++	+	++	+
liver	+	+	+++	+
small intestine	++	+	++	+
spleen	+	+	+++	+
thymus	+	+	++	+
peripheral leukocyte	+	+	–	+
lymph node	+	+	++	+
bone marrow	+	+	+++	+
appendix	+	+	+	–
lung	+	+	+	+
trachea	+	+	+	–
placenta	+	+	+	+
fetal brain	+	+	+	+
fetal heart	+	+	–	+
fetal kidney	+	+	++	+
fetal liver	+	+	+++	–
fetal spleen	+	+	++	–
fetal thymus	+	+	+	+
fetal lung	+	+	+	+

[a] Expression levels of each gene is given relative to DNase I gene expression in adult pancreace as 100%: +++, over 60%; ++, between 30 and 60%; +, less than 30%; −, not detected.

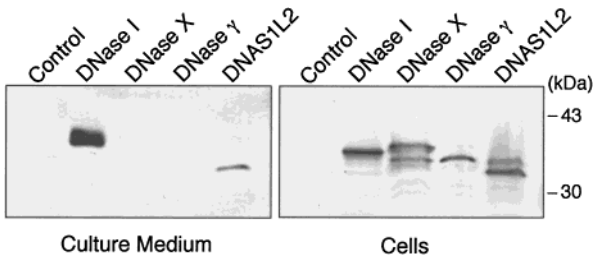

FIGURE 2: Western blot analyses of recombinant DNase I family DNases. 293 cells were transfected with each expression vector for DNase I family DNases as described under Materials and Methods. After the cells were cultured for 48 h, the culture medium and cells were collected separately and subjected to Western blot. Myc-His-tagged forms of DNase I family DNases, secreted into culture medium (left panel) or retained within the cells (right panel), were detected by Western blotting using anti-Myc antibody as described under Materials and Methods.

On the other hand, DNase X and DNase γ are detected only in the cellular fractions. DNase X was detected as two bands (39 and 35 kDa), and the apparent M_r of the lower band agrees well with the calculated M_r of 35 211. The upper band may include an *N*-linked sugar chain, because a potential glycosylation site is located at Asn 243 as indicated in Figure 1. DNase γ was detected as a single band with an apparent M_r of 36 kDa. This closely matches its calculated M_r of 36 618.

Characterization of the DNase Activities of DNase I Family Proteins. As shown in Figure 1, two His residues are found to be conserved among DNase I family proteins. Importantly, these His residues are shown to be essential for DNase I activity (*45*). Although the enzymatic activities of DNase X and DNAS1L2 have yet to be identified, the striking conservation of the active His residues suggests their DNase I-like divalent cation-dependent DNase activities. In addition, although the DNase I and DNase γ activities have been studied extensively, their properties were determined using different enzyme sources, purities, and assay systems. Thus, we cannot conclude that their enzymatic properties are really different. To resolve these problems, we examined the DNase activities by the same assay system using affinity-purified recombinant DNase I family proteins.

First, we analyzed the optimum pH for each DNase activity in the presence of Ca^{2+} and Mg^{2+}. To examine their endonuclease activities, we used supercoiled plasmid DNA as a substrate. As shown in Figure 3, DNase I, DNase X, and DNase γ activities were observed at neutral pH range with maxima at pH 6.8, 6.8, and 7.2, respectively, in Mops-NaOH buffer. Unexpectedly, a high DNAS1L2 activity was observed at acidic pH with a maximum at pH 5.6 under the same assay conditions (Figure 3, panel D). These four DNases were inactive in the absence of Ca^{2+} and Mg^{2+} regardless of the pH conditions (data not shown). Thus, all of the DNase I family proteins are shown to be divalent cation-dependent endonucleases. Furthermore, it is of note that DNAS1L2 is an acidic endonuclease, while DNase I, DNase X, and DNase γ are neutral endonucleases.

To obtain more information about the properties of the DNase I family DNases, we next examined their divalent cation requirements for DNase activities. DNase I and DNase X are activated by Ca^{2+} or Mg^{2+} alone (Figure 4, panels A and C), whereas, DNase γ and DNAS1L2 activities are scarcely observed in the presence of Ca^{2+} or Mg^{2+} (Figure 4, panels E and G). To examine the synergistic effect of Ca^{2+} and Mg^{2+}, assays were performed at various concentrations of Ca^{2+} in the presence of 3 mM Mg^{2+}. As shown in Figure 4, panels A, C, E, and G, all of the DNase I family DNases are synergisticaly activated by Ca^{2+} and Mg^{2+}. On the basis of these results, they are shown to be Ca^{2+}/Mg^{2+}-dependent endonucleases. In this study, we defined each DNase activity as that observed at the optimum pH in the presence of the optimum concentrations of Ca^{2+} and Mg^{2+} as 100%, and the activities observed under various other conditions are expressed as relative percentages.

In previous reports, DNase I and DNase γ were shown to be activated by a single divalent cation other than Ca^{2+} or Mg^{2+} (*1*−*3*, *10*−*12*). Therefore, we examined the effects of some other divalent cations on DNase I family DNases. Among the divalent cations tested, Mn^{2+} and Co^{2+} were found to activate all of the DNases. Although at most 50 to

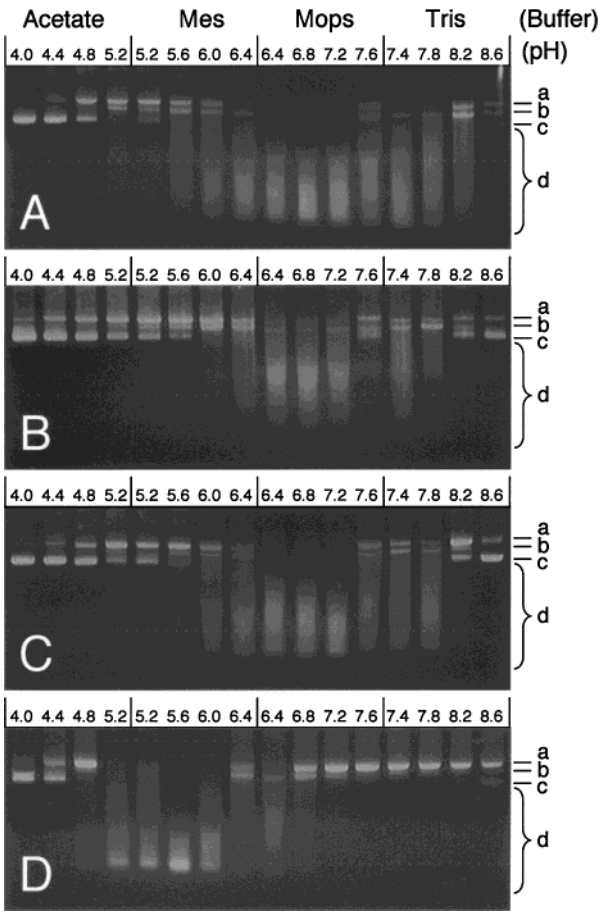

FIGURE 3: Effects of pH on DNase I family DNase activities. The activities of DNase I (A), DNase X (B), DNase γ (C), and DNAS1L2 (D) were assayed using supercoiled plasmid as described under Materials and Methods, except that the following buffers were used: acetate-NaOH (pH 4.0, 4.4, 4.8, and 5.2), Mes-NaOH (pH 5.2, 5.6, 6.0, and 6.4), Mops-NaOH (pH 6.4, 6.8, 7.2, and 7.6), and Tris-HCl (pH 7.4, 7.8, 8.2, and 8.6). The forms of plasmid DNA are indicated to the right of the panels; open coil (a), linear (b), supercoil (c), and degraded fragments (d).

60% activities were observed at optimum concentrations for DNase I, DNase X, and DNase γ (Figure 4, panels B, D, and F), DNAS1L2 exerted more than 200% activity in the presence of 10 mM Co^{2+} and 80% activity in the presence of 10 mM Mn^{2+} (Figure 4, panel H). In contrast to Mn^{2+} and Co^{2+}, no DNase activity was detected in the presence of up to 10 mM Ni^{2+} or Zn^{2+} (data not shown).

We next examined the effects of known DNase inhibitors on the DNase activities. G-actin, a specific inhibitor of DNase I (*46*), strongly inhibited DNase I (Figure 5A). Unexpectedly, DNase X was inhibited by G-actin at high concentrations (Figure 5, panel A). This is not nonspecific inhibition, because no effects were observed on DNase γ or DNAS1L2 activities at any dose of G-actin tested. The IC_{50} of G-actin for DNase I and DNase X activities are estimated to be 2 and 50 μg/mL, respectively. The inhibition efficiency of aurintricarboxylic acid (ATA), a general inhibitor of nucleases (*47*), on each DNase was found to be quite different. DNase γ and DNAS1L2 were strongly inhibited by ATA, whereas DNase I and DNase X were relatively resistant (Figure 5, panel B). The ATA concentrations to give IC_{50} for DNase I, DNase X, DNase γ, and DNAS1L2 are 50, 38, 0.35, and 0.4 μM, respectively. In previous reports, DNase I and DNase γ activities were shown to be suppressed by

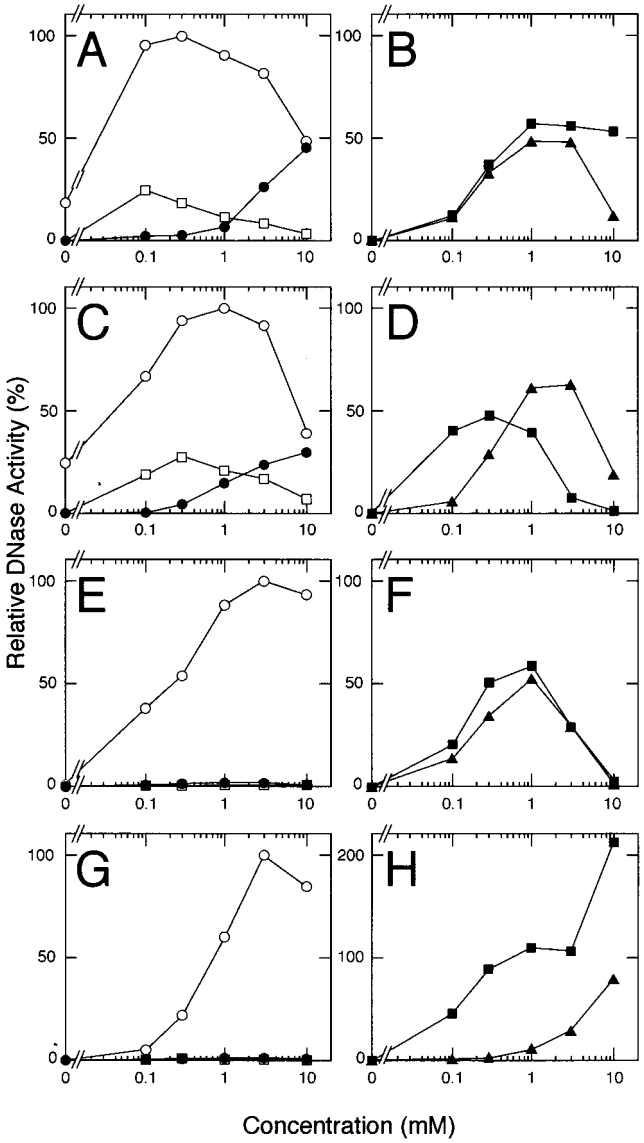

FIGURE 4: Effects of divalent cations on DNase I family DNases. The activities of DNase I (A and B), DNase X (C and D), DNase γ (E and F), and DNAS1L2 (G and H) were measured using linear plasmid DNA as described under Materials and Methods in the presence of $CaCl_2$ (□), $MgCl_2$ (●), $CaCl_2$ (in combination of 3 mM $MgCl_2$) (○), $MnCl_2$ (▲), or $CoCl_2$ (■). Values are the averages of the results obtained from three independent experiments.

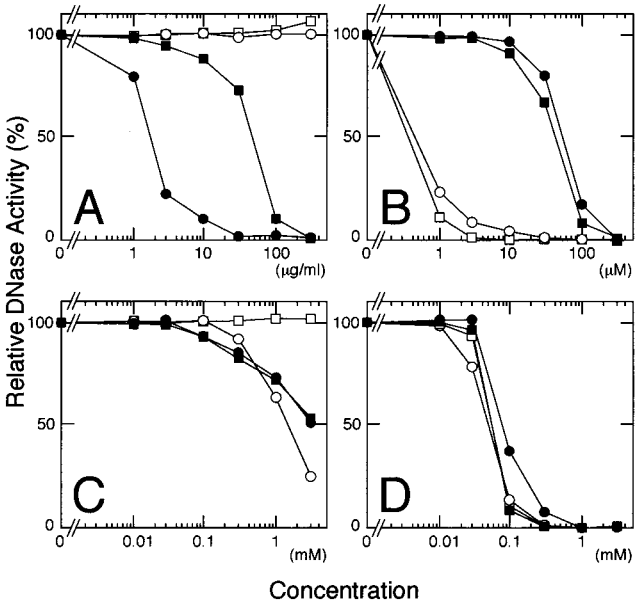

FIGURE 5: Effects of DNase inhibitors on DNase I family DNases. The activities of DNase I (●), DNase X (■), DNase γ (○), and DNAS1L2 (□) were measured using linear plasmid DNA as described under Materials and Methods in the presence of the indicated concentrations of (A) G-actin, (B) ATA, (C) $NiCl_2$, or (D) $ZnCl_2$. Data represent averages of the results obtained from three independent experiments.

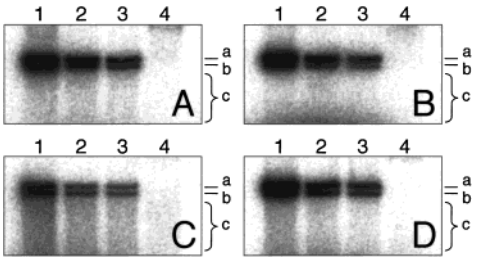

FIGURE 6: End-labelings of DNA fragments generated by DNase I family DNases. Supercoiled plasmid DNAs digested by DNase I (A), DNase X (B), DNase γ (C), and DNAS1L2 (D) were subjected to 3′- (lanes 1 and 2) or 5′- (lanes 3 and 4) end-labeling with (lanes 1 and 3) or without (lanes 2 and 4) pretreatment with alkaline phosphatase as described under Materials and Methods. DNA was separated by 1.0% agarose gel electrophoresis, transferred to nylon membranes, and analyzed by autoradiography. The forms of plasmid DNA are indicated to the right of the panels: open coil (a), linear (b), and degraded fragments (c).

divalent-metal ions (*10*−*12*, *14*). Therefore, we tested the effects of Ni^{2+} and Zn^{2+} on the DNase I family DNases. Although Ni^{2+} inhibited DNase I, DNase X, and DNase γ with IC_{50} of 3, 3, and 1.4 mM, respectively, no effect was observed on DNAS1L2 activity (Figure 5, panel C). In contrast to Ni^{2+}, Zn^{2+} inhibited all the DNases with almost the same efficiency (Figure 5, panel D). The IC_{50} of Zn^{2+} for DNase I, DNase X, DNase γ, and DNAS1L2 activities are estimated to be 80, 60, 50, and 60 μM, respectively.

Mode of DNA Hydrolysis. DNases can be divided into two classes on the basis of their mode of DNA hydrolysis: one includes DNases producing 3′-OH/5′-P cleaving ends and the other includes those that produce 3′-P/5′-OH ends. Although DNase I and DNase γ have been shown to belong to the former class (*1*, *10*), the mode of DNA hydrolysis of DNase X and DNAS1L2 are unknown. Since elucidation of the mode of DNA hydrolysis of DNase I family DNases is important for understanding their physiological importance, we performed 3′- and 5′- end-labeling of the DNA cleaved by each DNase. As shown in Figure 6, panels B and C, the 3′-ends of the DNA fragments produced by DNase X or DNAS1L2 were labeled regardless of alkaline phosphatase pretreatment. In contrast, the 5′-ends could be labeled only after the removal of the phosphoryl groups. These labeling patterns are the same as those by DNase I or DNase γ (Figure 6, panels A and C). These observations clearly show that all of the DNase I family DNases catalyze DNA hydrolysis to produce 3′-OH/5′-P ends.

Involvement of DNase I Family DNases in Apoptosis. In recent studies, one physiological role of DNase I and DNase γ has been predicted to be the catalysis of DNA fragmentation during apoptotic cell death (*14*−*20*). Furthermore, DNase γ has been shown to be activated by apoptotic stimuli and produce oligonucleosomal DNA ladder in its transfected cells (*17*, *19*). Because the cleavage ends of DNA fragments (3′-OH/5′-P) produced during apoptosis in vivo (*10*) are the

same as those digested by the DNase I family DNases in vitro (Figure 6), we examined whether all of the DNase I family DNases can be activated and catalyze nucleosomal DNA fragmentation during apoptosis. In this study, we used HeLa S3 cells as a transfection host because (i) although a slight expression of DNase X mRNA is detected, little endogenous expression of the other DNase I family genes are observed (Figure 7A) and (ii) they die by apoptosis without extensive oligonucleosomal DNA fragmentation in response to various apoptotic stimuli (Figure 7, panel C) (*17*, *19*, *30*, *33*). Therefore, HeLa S3 cells are considered to be a suitable host for functional analysis of the DNase I family DNases. The existence of DNase II and CAD mRNAs could be detected by RT-PCR (Figure 8, panel A). However, Northern blot analyses has shown that their expression levels are quite low in HeLa S3 cells (*30*, *33*), and this is thought to be a cause for the absence of extensive apoptotic DNA fragmentation in HeLa S3 cells (*30*, *33*). In the following experiments, the same intracellular protein levels for each ectopic DNase were confirmed by Western blot analysis with anti-Myc antibody (data not shown). The transfection of HeLa S3 cells with expression vectors for each DNase causes no loss of viability or spontaneous DNA fragmentation (Figure 7, panel C), indicating that the transient expression of the DNases themselves has no toxic or apoptosis inducing effect on the cells. This is supported by the observation that reactivities to annexin V and propidium iodide (PI) in each transfectant are the same as those of control cells (Figure 7, panel B). We next examined the effects of each DNase on TNF-α-induced apoptosis. After 12 h continuous treatment with TNF-α/Act D, about 70% of the cells turned to be reactive to annexin V and 20% to PI staining (Figure 7, panel B). Importantly, apoptosis indexes of each DNase expressing cells are almost the same as those of control cells, indicating that the ectopic expression of DNase I family DNases has essentially no effect on cell death. As shown in Figure 7, panel D, nucleosomal DNA fragmentation was scarcely observed in DNase I, DNase X, or DNAS1L2 transfected cells. Although slight smearing was observed in DNase I cells, the extents of DNA degradation in these three transfectants were almost the same as that observed in control cells. In contrast to DNase I, DNase X, and DNAS1L2, clear DNA fragmentation into oligonucleosomal ladder was observed in DNase γ transfected cells (Figure 7, panel D). The same results were obtained when camptothecin, adriamycin, and C2-ceramide were used as apoptosis inducers (data not shown). On the basis of these results, among DNase I family DNases, DNase γ is the sole DNase that is activated by apoptotic stimuli and catalyzes internucleosomal DNA fragmentation in mammalian cells.

Nuclear Translocation of DNase γ during Apoptosis. To understand the activation mechanism of DNase γ during apoptosis, we expressed DNase γ as a GFP fusion protein and determined the subcellular distribution. We fused GFP to the C-terminus of DNase γ, because DNase I family DNases contain precursor peptides in their N-termini (Figure 1), and GFP fused to their N-termini would interfere with the collect processing and distribution of the DNases. As shown in Figure 8, panel A, fluorescence microscopic analysis revealed that DNase γ was located around the perinuclear region in living (nonapoptotic) cells. Importantly, DNase γ was translocated into the nucleus when apoptosis

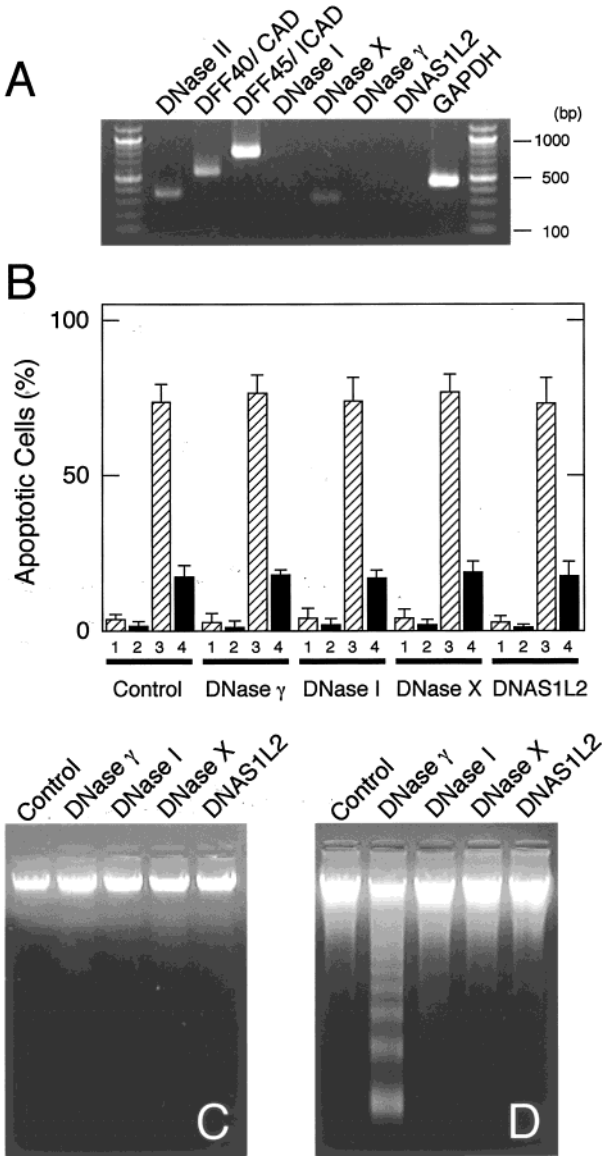

FIGURE 7: Effects of ectopic expression of DNase I family DNases on TNF-α-induced apoptosis in HeLa S3 cells. (A) Endogenous expression levels of DNase I family genes in HeLa S3 cells. Total RNA was prepared from HeLa S3 cells and PT-PCR was performed as described under Materials and Methods. The identities of the PCR products are indicated at the top of each lane. Results for DNase II, DFF40/CAD, DFF45/ICAD, and GAPDH were shown for comparison. (B) TNF-α-induced apoptosis in HeLa S3 cells transfected with DNase I family DNase expression vectors. Apoptosis was induced by TNF-α (1 ng/mL)/Act D (0.3 μg/mL) treatment for 12 h. Percentages of apoptotic cells in nontreated (lanes 1 and 2) and TNF-α/Act-D-treated (lanes 3 and 4) samples were analyzed by annexin V binding assay (lanes 1 and 3, striped bars) and PI staining (lanes 2 and 4, closed bars), respectively, as described under Materials and Methods. Values are the averages of three independent experiments and are shown with standard deviation. The identities of DNase expressed in the cells are indicated at the bottom. Cells transfected with empty vector were used as control. (C and D) Apoptotic DNA fragmentation in HeLa S3 cells transfected with DNase I family DNase expression vectors. Apoptosis was induced by TNF-α (1 ng/mL)/Act D (0.3 μg/mL) treatment in each expression vector transfected cells. After 12 h of incubation, nontreated (C) and TNF-α/Act-D-treated (D) cells were harvested and DNA fragmentation was observed as described under Materials ans Methods. The identities of DNase expressed in the cells are indicated at the top of each lane. Cells transfected with empty vector were used as control.

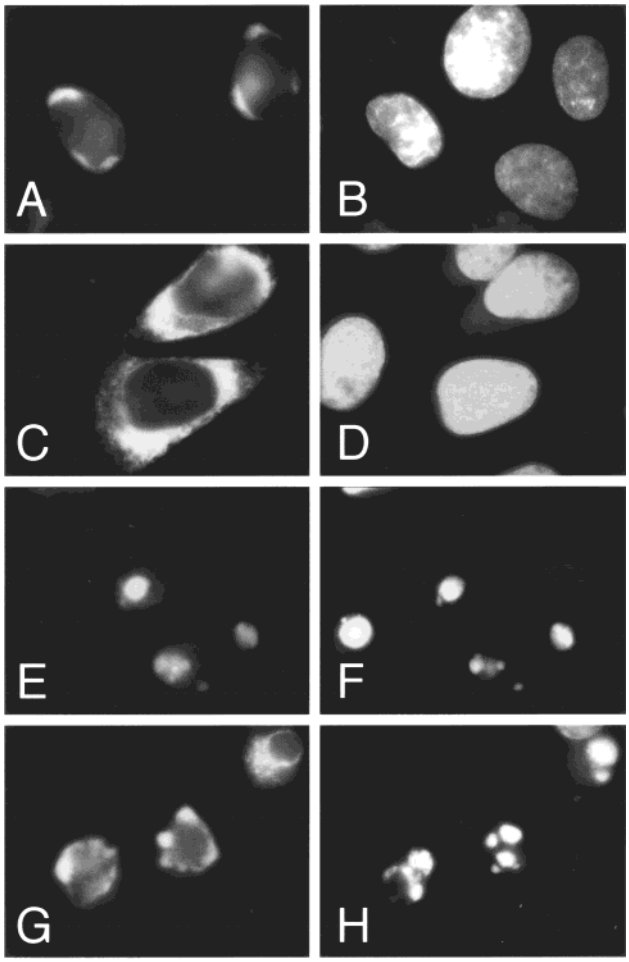

FIGURE 8: Subcellular localization of DNase γ expressed in HeLa S3 cells. Apoptosis was induced in the cells transfected with phDNase γ-GFP (A, B, E, and F) or phDNAS1L2-GFP (C, D, G, and H) by addition of TNF-α (1 ng/mL) and Act D (0.3 μg/mL). After the cells were cultured for 12 h, nontreated (A, B, C, and D) and TNF-α/Act-D-treated (E, F, G, and H) cells were fixed, stained with Hoechst 33258, and the fluorescence of GFP (A, C, E, and G) and Hoechst (B, D, F, and H) was monitored by fluorescence microscopy as described under Materials and Methods.

was induced by TNF-α/Act D treatment (Figure 8, panel C). We performed the same experiments using DNAS1L2, which has no ability to produce DNA fragmentation during apoptosis (Figure 7, panel D). In living cells, DNAS1L2 was found predominantly in the cytoplasm with a punctate pattern of distribution, suggesting the likely cellular compartments of DNAS1L2 to be ER and Golgi complex. This prediction is supported by the observation that DNAS1L2 is secreted into the culture medium when expressed in 293 cells (Figure 2). In contrast to DNase γ, nuclear translocation of DNAS1L2 could not be observed during apoptosis (Figure 8, panel G). These observations suggest that the nuclear translocation of DNase γ is not a nonspecific result occurring as a consequence of apoptotic nuclear condensation but is a specific feature of DNase γ.

DISCUSSION

In this study, we purified and characterized human DNase I family DNases, DNase I, DNase X, DNase γ, and DNAS1L2, generated as Myc-His tagged recombinant proteins through the same procedures. This is the only comparative characterization of mammalian DNase I-type endonucleases. On the basis of poly A(+) RNA dot blot analysis, DNase I family genes are shown to be expressed with different tissue specificities and are suggested to play unique physiological roles. Western blot analysis of the DNase I family proteins revealed that their extra- and intracellular distributions are quite different (Figure 2). This clearly indicates that the conserved hydrophobic precursor peptides do not always direct them to the secreting pathways. The possible domains responsible for the intracellular retention of DNase γ and DNase X are thought to be their C-terminal stretches, which are not found in DNase I or DNAS1L2, because a DNase γ mutant deleted in the C-terminal basic domain is effectively secreted in the same manner as DNase I (our unpublished observation). Although the elucidation of the precise cellular distributions and the traffic mechanisms must await further studies, our results suggest that the DNase I family proteins evolved originally as secretory proteins, and through the acquisition of C-terminal extradomains, DNase γ and DNase X came to be retained within cells and to play specific roles distinct from those of DNase I or DNAS1L2.

We next examined the enzymatic properties of the DNase I family proteins using affinity-purified recombinants and revealed their divalent cation-dependent endonuclease activities. To generate recombinant DNases, we chose a mammalian expression system because several lines of evidence suggest that some eukaryotic posttranslational modifications are essential for their biosynthesis: (i) removal of the precursor peptide is essential for the activity of DNase γ protein (*17*) and (ii) DNase I has two *N*-linked glycosylation sites and bovine pancreatic DNase I is shown to contain a single oligosaccharide at Asn18 (*42*).

The enzymatic properties of DNase X were found to be similar to those of DNase I. Both DNases are activated by Ca^{2+} or Mg^{2+} alone, inhibited by G-actin, and are relatively insensitive to ATA. The inhibition of DNase X by G-actin is an unexpected result (Figure 5), because the actin binding sites determined in DNase I are not well-conserved in DNase X. In the previous studies, actin binding sites, E13, H44, D53, Y65, V67, and E69 were determined in bovine DNase I (*48*), and by comparison, the corresponding residues in DNase X are predicted to be L13, S44, R53, T66, S68, and P69, respectively. Although we can give no clear explanation for the inhibition mechanism of DNase X by G-actin, some of the substituted amino acids are considered to be partially compatible with actin binding, and this may account for the different IC_{50} values between DNase I and DNase X.

DNAS1L2 is revealed to have a Ca^{2+}/Mg^{2+}-dependent acidic endonuclease activity (Figure 3). It is of note that this is the first report of a mammalian divalent cation-dependent acidic DNase. Besides its optimum pH, DNAS1L2 has a unique divalent cation requirement, namely, its activation by Mn^{2+} and Co^{2+} (Figure 4). These divalent cations exert about half the activation efficiencies of Ca^{2+}/Mg^{2+} on other DNase I family members, whereas Mn^{2+} activates DNAS1L2 to almost the same extent as Ca^{2+}/Mg^{2+}. Furthermore, a more than 2-fold activation of DNAS1L2 is observed by Co^{2+}. Interestingly, a biphasic activation of DNAS1L2 by Co^{2+} was observed: the first peak is observed at 1 mM, is lower at 3 mM, and high again at 10 mM. The molecular basis of this phenomenon is at present unknown; however, we confirmed that the observation is reproducible by performing

more precise dose effects between 1 and 10 mM Co^{2+} (data not shown).

ATA has long been used as a general nuclease inhibitor. We clearly showed that the sensitivities of the DNase I family DNases for ATA are quite different (Figure 5, panel B). Although the reason for these differences remains unknown, the sugar chains in DNase molecules may produce different sensitivities to ATA. In contrast to ATA, the inhibitory effects of Zn^{2+}, which has been believed to inhibit specific DNases, were shown to be almost the same for all DNase I family DNases (Figure 5, panel C).

Among the DNase I family DNases, DNase γ has been examined with regard to apoptotic DNA fragmentation in mammalian cells: the ectopic expression of DNase γ itself has no effect on the viability of transfected cells; however, DNase γ is activated by various apoptotic stimuli and catalyzes nucleosomal DNA fragmentation during apoptosis (*17*, *19*). In the present study, we examined the involvement of DNase I family DNases in apoptotic DNA fragmentation in HeLa S3 cells, and, as a result, DNase γ is shown to be the sole DNase capable of producing DNA ladder during apoptosis in this expression system (Figure 7). Importantly, these observations also indicate that the apoptotic activation of DNase γ is not an artifact caused by the ectopic expression of active DNase in cells.

At present, the well-known apoptotic DNase is CAD/DFF-40/CPAN (*32*−*35*). CAD has been shown to be inactivated by complexing with its inhibitor ICAD/DFF-45 in living cells, and during apoptosis, CAD is activated by the caspase-mediated cleavage of ICAD and catalyzes apoptotic DNA fragmentation (*32*−*34*). Although the activation mechanism of DNase γ has yet to be elucidated, our present study provides an important clue to understand its activation mechanism during apoptosis. Fluorescence microscopic analysis revealed that DNase γ-GFP was translocated from the perinuclear region into the nucleus during apoptosis (Figure 8), suggesting that the nature of the apoptotic activation of DNase γ is its nuclear translocation. This is consistent with our previous observation that DNase γ activity was accumulated in the nuclear fraction during apoptosis in HeLa S3/DNase γ stable transfectant (*17*). The nuclear translocation of DNase γ is likely to occur depending on its NLS (Figure 1) and considered to be an important step for the function of DNase γ in apoptosis. As mentioned in Results, existence of NLS is a unique feature of DNase γ, and this may give an account for the observation that DNase γ is the solo DNase that can produce apoptotic DNA fragmentation among DNase I family DNases (Figure 7, panel D).

On the basis of the molecular structure of DNase γ, one possible pathway for its biosynthesis and apoptotic activation mechanism is as follows. During de novo synthesis, the nascent chain of DNase γ protein is translocated into the endoplasmic reticulum (ER) depending on its hydrophobic precursor peptide. After removal of the peptide by some signal peptidase, the mature DNase γ is transported to the nuclear envelope and stored in its inner space until the onset of apoptosis. When cells are exposed to some apoptotic stimuli, DNase γ is released from the nuclear envelope, is translocated to the nucleus depending on its NLS, and cleaves genomic DNA into oligonucleosomal fragments.

Recent studies have revealed that many apoptosis-promoting factors are stored or located in some subcellular compartments and released to the cytoplasm when apoptosis is triggered (*49*−*51*). Release of cytochrome *c* from the mitochondria is regulated by the Bcl-2 family proteins, and one of their molecular targets has recently been identified as voltage-dependent anion channel (VDAC): Bcl-x closes the VDAC, whereas Bax and Bak promote opening of the channel so that cytochrome *c* is released to the cytoplasm (*50*, *52*). Release of DNase γ from the nuclear envelope may be controlled by some mechanisms similar to those for cytochrome *c* release. Furthermore, this may give an answer for the question of why Bcl-2 family proteins are located in the nuclear envelope (*51*).

In this study, we demonstrated that only DNase γ is activated by apoptotic stimuli and capable of producing DNA fragmentation among the four DNase I family DNases. However, we cannot exclude the possible participation of other members under some apoptotic conditions. For instance, it may be interesting to examine the involvement of DNAS1L2 in apoptosis when intracellular acidification occurs. Under such conditions, pH-sensitive endonucleases have been considered candidates for the DNase responsible for apoptotic DNA fragmentation (*53*, *54*). On the basis of its properties, DNAS1L2 is thought to be the most likely candidate, because it prefers acidic pH for its activity, and both of the DNA fragments produced by DNAS1L2 in vitro and during apoptosis in vivo have the same 3′-OH/5′-P ends (*10*). Furthermore, the participation of DNase I has been reported during apoptosis in spermatocytes and prostate epithelial cells (*15*, *16*). Thus, it is possible that multiple DNases, including DNase II, L-DNase II, and CAD, are involved in apoptosis and that their activations differ with the cell type, status (growing, undifferentiating, and differentiating), and/or apoptotic stimuli.

In summary, we have described the tissue-specific gene expression and physical and enzymatic properties of the four human DNase I family DNases. In addition, we examined their possible involvement in apoptosis and found that only DNase γ is activated by apoptotic stimuli and produce nucleosomal DNA fragmentation in mammalian cells. Our results provide some important clues for understanding the physiological and pathological importance of DNase I family endonucleases.

ACKNOWLEDGMENT

We thank Miss M. Tanaka for her excellent technical assistance.

REFERENCES

1. Laskowski, M. (1971) in *The Enzymes* (Boyer, P. D., Landy, H., and Myrbäck, K., Eds) Vol. 4, pp 289−311, Academic Press, New York.
2. Price, P. A. (1975) *J. Biol. Chem. 250*, 1981−1986.
3. Campbell, V. W., and Jackson, D. A. (1980) *J. Biol. Chem. 255*, 3726−3735.
4. Shak, S., Capon, D. J., Hellmiss, R., Marsters, S. A., and Baker, C. L. (1990) *Proc. Natl. Acad. Sci. U.S.A. 87*, 9188−9192.
5. Pergolizzi, R., Appierto, V., Bosetti, A., DeBellis, G. L., Rovida, E., and Biunno, I. (1996) *Cell Death Differ. 3*, 199−206.
6. Coy, J. F., Velhagen, I., Himmele, R., Delius, H., Poustka, A., and Zentgraf, H. (1996) *Gene 168*, 267−270.

7. Shiokawa, D., Hirai, M., and Tanuma, S. (1998) *Apoptosis 3*, 89−95.
8. Rodriguez, A. M., Rodin, D., Nomura, H., Morton, C. C., Weremowicz, S., and Schneider, M. C. (1997) *Genomics 42*, 507−513.
9. Baron, W. F., Pan, C. Q., Spencer, S. A., Ryan, A. M., Lazarus, R. A., and Baker, K. P. (1998) *Gene 215*, 291−301.
10. Shiokawa, D., Ohyama, H., Yamada, T., Takahashi, K., and Tanuma, S. (1994) *Eur. J. Biochem. 226*, 23−30.
11. Shiokawa, D., Iwamatsu, A., and Tanuma, S. (1997) *Arch. Biochem. Biophys. 346*, 15−20.
12. Shiokawa, D., Ohyama, H., Yamada, T., and Tanuma, S. (1997) *Biochem. J. 326*, 675−681.
13. Appierto, V., Bardella, L., Vijayasarathy, C., Avadhani, N., Sgaramella, V., and Biunno, I. (1997) *Gene 188*, 119−122.
14. Peitsch, M. C., Polzar, B., Stepham, H., Crompton, T., MacDonald, H. R., Mannherz, H. G., and Tshopp, J. (1993) *EMBO J. 12*, 371−377.
15. Rauch, F., Polzar, B., Stephan, H., Zanotti, S., Paddenberg, R., and Mannherz, H. G. (1997) *J. Cell Biol. 137*, 909−923.
16. Stephan, H., Polzar, B., Rauch, F., Zanotti, S., Ulke, C., and Mannherz, H. G. (1996) *Histochem. Cell Biol. 106*, 383−393.
17. Shiokawa, D., and Tanuma, S. (1998) *Biochem. J. 332*, 713−720.
18. Liu, Q. Y., Pandey, S., Singh, R. K., Lin, W., Ribecco, M., Borowy-Borowski, H., Smith, B., LeBlanc, J., Walker, P. R., and Sikorska, M. (1998) *Biochemistry 37*, 10134−10143.
19. Yakovlev, A. G., Wang, G., Stoica, B. A., Simbulan-Rosenthal, C. M., Yoshihara, K., and Smulson, M. E. (1999) *Nucleic Acids Res. 27*, 1999−2005.
20. Kimura, C., Zhao, Q., Kondo, T., Amatsu, M., and Fujiwara, Y. (1998) *Exp. Cell Res. 239*, 411−422.
21. Kerr, J. F. R., Wyllie, A. H., and Currie, A. R. (1972) *Br. J. Cancer 26*, 239−257.
22. Fadeel, B., Orrenius, S., and Zhivotovsky, B. (1999) *Biochem. Biophys. Res. Commun. 266*, 699−717.
23. Ellis, R. E., Jacobson, D. M., and Horvitz, H. R. (1991) *Genetics 129*, 79−94.
24. Wu, Y. C., Stanfield, G. M., and Horvitz, H. R. (2000) *Genes Dev. 14*, 536−548.
25. Odaka, C., and Mizuochi, T. (1999) *J. Immunol. 163*, 5346−5352.
26. McIlroy, D., Tanaka, M., Sakahira, H., Fukuyama, H,. Suzuki, M., Yamamura, K., Ohsawa, Y., Uchiyama, Y., and Nagata, S. (2000) *Genes Dev. 14*, 549−558.
27. Wyllie, A. H. (1980) *Nature 284*, 555−556.
28. Arends, M. J., Morris, R. G., and Wyllie, A. H. (1990) *Am. J. Pathol. 136*, 593−601.
29. Barry, M. A., and Eastman, A. (1993) *Arch. Biochem. Biophys. 300*, 440−450.
30. Krieser, R. J., and Eastman, A. (1998) *J. Biol. Chem. 273*, 30909−30914.
31. Torriglia, A., Perani, P., Brossas, J. Y., Chaudun, E., Treton, J., Courtois, Y., and Counis, M.-F. (1998) *Mol. Cell. Biol. 18*, 3612−3619.
32. Enari, M., Sakahira, H., Yokoyama, H., Okawa, K., Iwamatsu, A., and Nagata, S. (1998) *Nature 391*, 43−50.
33. Mukae, N., Enari, M., Sakahira, H., Fukuda, Y., Inazawa, J., Toh, H., and Nagata, S. (1998) *Proc. Natl. Acad. Sci. U.S.A. 95*, 9123−9128.
34. Liu, X., Zou, H., Slaughter, C., and Wang, X. (1997) *Cell 89*, 175−184.
35. Halenbeck, R., MacDonald, H., Roulson, A., Chen, T. T., Conroy, L., and Williams, L. T. (1998) *Curr. Biol. 8*, 537−540.
36. Sakahira, H., Enari, M., and Nagata, S. (1998) *Nature 391*, 96−99.
37. Zhang, J., Wang, X., Bove, K. E., and Xu, M. (1999) *J. Biol. Chem. 274*, 37450−37454.
38. Wagner, J. A., Chao, A. C., and Gardner, P. (1995) *Annu. Rev. Pharmacol. Toxicol. 35*, 257−276.
39. Shak, S. (1995) *Chest 107*, 65−70.
40. Shiokawa, D., and Tanuma, S. (1999) *Nucleic Acids Res. 27*, 4083−4089.
41. Tanuma, S., and Shiokawa, D. (1994) *Biochem. Biophys. Res. Commun. 203*, 789−797.
42. Paudel, H. K., and Liao, T. H. (1986) *J. Biol. Chem. 261*, 16012−16017.
43. Malferrari, G., Mazza, U., Tresoldi, C., Rovida, E., Nissim, M., Mirabella, M., Servidei, S., and Biunno, I. (1999) *Exp. Mol. Pathol. 66*, 123−130.
44. Nishikawa, A., Gregory, W., Frenz, J., Cacia, J., and Kornfeld, S. (1997) *J. Biol. Chem. 272*, 19408−19412.
45. Jones, S. J., Worrall, A. F., and Connolly, B. A. (1996) *J. Mol. Biol. 264*, 1154−1163.
46. Kreuder, V., Dieckhoff, J., Sittig, M., and Mannherz, H. G. (1984) *Eur. J. Biochem. 139*, 389−400.
47. Hallick, R. B., Chelm, B. K., Gray, P. W., and Orozco, E. M., Jr. (1977) *Nucleic Acids Res. 4*, 3055−3064.
48. Kabsch, W., Mannherz, H. G., Suck, D., Pai, E. F., and Holmes, K. C. (1990) *Nature 347*, 37−44.
49. Green, D. R., and Reed, J. C. (1998) *Science 281*, 1309−1312.
50. Tsujimoto, Y., and Shimizu, S. (2000) *FEBS Lett. 466*, 6−10.
51. Zamzami, N., Brenner, C., Marzo, I., Susin, S. A., and Kroemer, G. (1998) *Oncogene 16*, 2265−2282.
52. Shimizu, S., Narita, M., and Tsujimoto, Y. (1999) *Nature 399*, 483−487.
53. Barry, M. A., Reynolds, J. E., and Eastman, A. (1993) *Cancer Res. 53*, 2349−2357.
54. Perez-Sala, D., Collado-Escobar, D., and Mollinedo, F. (1995) *J. Biol. Chem. 270*, 6235−6242.

BI001041A